

**KAWASAKI STEEL TECHNICAL REPORT**

No.14 ( March 1986 )

*Special Issue on Stainless Steels*

---

**Hot Workability of Austenitic Stainless Steels Containing  
Delta-Ferrite**

Tatsuo Kawasaki, Isao Takada, Hiroshi Ohtsubo, Shigeharu Suzuki

---

Synopsis :

Hot workability of austenitic stainless steels, which have problems of cracking when they are hot rolled, is studied. Sulfur has a great effect on hot workability and decreases ductility of steels at around 1050°C during cooling from the slab reheating temperature. For steel containing little delta-ferrite, the ductility increases again as the temperature decreases. For steels containing delta-ferrite, however, ductility does not increase again. Then, the temperature range of reduced ductility for these steels expands widely towards lower temperatures. The effects of S and delta-ferrite on hot workability are discussed. Hot workability of these steels are improved remarkably by eliminating the effect of S. Problems of cracking during hot working can be solved completely by reducing S content to below about 10 ppm and/or with the addition of Ca or REM.

(c)JFE Steel Corporation, 2003

**The body can be viewed from the next page.**

# Hot Workability of Austenitic Stainless Steels Containing Delta-Ferrite\*



Tatsuo Kawasaki  
Senior Researcher,  
Stainless Steel Lab.,  
I & S Research Labs.



Isao Takada  
Senior Researcher,  
Chita Research Dept.,  
I & S Research Labs.



Hiroshi Ohtsubo  
Senior Researcher,  
Plate Lab.,  
I & S Research Labs.



Shigeharu Suzuki  
Chief of Stainless  
Steel Lab., I & S  
Research Labs.

## Synopsis:

Hot workability of austenitic stainless steels, which have problems of cracking when they are hot rolled, is studied. Sulfur has a great effect on hot workability and decreases ductility of steels at around 1 050°C during cooling from the slab reheating temperature. For steel containing little delta-ferrite, the ductility increases again as the temperature decreases. For steels containing delta-ferrite, however, ductility does not increase again. Then, the temperature range of reduced ductility for these steels expands widely towards lower temperatures.

The effects of S and delta-ferrite on hot workability are discussed.

Hot workability of these steels are improved remarkably by eliminating the effect of S. Problems of cracking during hot working can be solved completely by reducing S content to below about 10 ppm and/or with the addition of Ca or REM.

trating the sound portion of the strip may cause rolled-in defects or holes, and requiring additional grinder processing and leading to lower hot-rolled strip yield. In  $\alpha$ - $\gamma$  duplex stainless steel, surface defects occurred with seamless pipe made by the Mannesmann plug mill

## 1 Introduction

In order to satisfy higher performance and material properties requirements, makers are increasingly turning to high alloy steels. At the same time, to minimize costs, the production of large slabs by continuous casting is being adopted. The combination of these two practices frequently gives rise to cracking problems during the hot rolling of austenitic and  $\alpha$ - $\gamma$  duplex stainless steels, in particular those containing  $\delta$ -ferrite in the range of 20-30% at elevated temperatures. For example, in 17-7 PH (SUS 631) and single-layer overlay welding electrode materials, edge cracks, as shown in **Photo 1**, are frequently observed. Torn edge cracking deep pene-

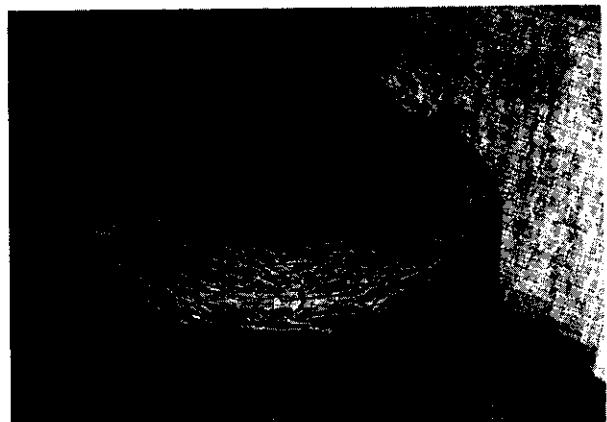


Photo 1 Edge crack of 17-7 PH hot strip

\* Originally published in *Kawasaki Steel Giho*, 17(1985)3, pp. 306-314

method, and edge cracks, such as those with the 17-7 PH, were observed in rolled strip. Thus, cracking during hot rolling presents the most serious problem in the production process for steels of these types.

It is generally thought that  $\delta$ -ferrite has a detrimental effect on hot workability, and that ductility is lowest when the austenite matrix contains 20-30%  $\delta$ -ferrite.<sup>1)</sup> When the  $\delta$ -ferrite contents matches more than 50%, that is, when the austenite phase is included in the ferrite phase, ductility becomes better than that with a single austenite phase. These facts are explained by the difference in high temperature strength and ductility of these phases. Also, it is known that high temperature ductility is affected by impurity elements such as S, P, and O, and their stabilizing elements, such as Ca, REM, and Al.<sup>2)</sup> In austenitic stainless steel of ordinary composition,  $\delta$ -ferrite content is large at high temperatures, and decreases as temperature decreases. Since cracking during hot rolling occurs as the rolling proceeds and the temperature drops, changes in  $\delta$ -ferrite amount must be considered when the temperature dependence of ductility is studied.

In this report, the hot workability of austenitic stainless steels is investigated, mainly with regard to the effect

of S, which is considered to have the strongest influence on hot workability; changes in  $\delta$ -ferrite amount are also studied.

## 2 Experimental

Experiments were performed mainly on 17-7 PH stainless steel. An overlay electrode material KWB309NB (24%Cr-13%Ni-1%Nb) and  $\alpha$ - $\gamma$  duplex stainless steel (22%Cr-5.5%Ni-3%Mo) were also used. Fully austenitic stainless steel SUS 310S was taken as a reference. Test specimens were cut from 50 kg vacuum melted ingots and commercial continuously cast slabs. Chemical compositions of specimens are shown in Table 1.

Hot ductilities were estimated from the reduction of area (RA) in a high temperature-high speed tensile test using a GLEEBLE 1 500 testing machine. The Gleeble test piece was 6.4 mm in diameter and about 20 mm in uniformly heated length. The test was performed on specimens with as-cast structure and those with hot rolled structure of 90% reduction after heating for 2 hours at 1 250°C. As-cast specimens were cut so as to include the surface side columnar structure. The

Table 1 Chemical compositions of specimens

(wt %)

		C	Si	Mn	P	S	Cr	Ni	Mo	Al	Nb	Ca	REM	N	O	$\delta_{\text{est}}^*$
17-7PH	50 kg ingot	0.069	0.42	0.74	0.024	0.0020	17.43	7.38	0.11	0.92	—	—	—	0.029	0.0007	24.0
		0.073	0.41	0.74	0.022	0.0028	17.53	7.46	0.11	0.99	—	—	—	0.029	0.0022	25.3
		0.076	0.41	0.74	0.024	0.0007	17.86	7.02	0.11	1.09	—	0.0030	—	0.028	0.0015	29.1
	Commercial CC slab	0.078	0.48	0.70	0.024	0.0011	16.79	7.20	0.03	1.06	—	—	—	0.016	0.0016	25.8
		0.061	0.53	0.72	0.029	0.0015	17.18	7.16	0.10	0.89	—	—	—	0.074	0.0019	21.0
		0.078	0.44	0.70	0.025	0.0110	16.77	7.15	0.10	1.11	—	—	—	0.024	0.0008	26.0
KWB 309NB	50 kg ingot	0.032	0.50	1.89	0.025	0.0012	23.15	12.96	0.10	0.020	1.08	—	—	0.025	0.0050	14.5
		0.023	0.45	2.03	0.025	0.0010	24.04	13.05	0.10	0.046	1.06	0.0038	—	0.027	0.0053	17.2
		0.025	0.46	2.02	0.010	0.0011	24.23	13.06	0.09	0.040	1.08	0.0024	—	0.025	0.0051	17.8
		0.024	0.44	2.04	0.024	0.0008	23.96	13.04	0.10	0.040	1.05	0.0024	—	0.033	0.0066	16.3
		0.023	0.56	2.04	0.025	0.0017	23.23	12.09	0.10	0.060	1.15	—	—	0.029	0.0079	17.5
KWB 309	50 kg ingot	0.013	0.12	1.56	0.016	0.0008	21.11	9.49	—	0.043	—	—	—	0.012	—	15.9
		0.014	0.12	1.50	0.015	0.0005	21.92	9.26	—	0.051	—	—	0.03	0.023	—	18.2
310S	50 kg ingot	0.062	0.85	1.50	0.023	0.0012	24.75	18.94	0.59	0.0030	—	—	—	0.037	0.0060	—
		0.062	0.80	1.64	0.023	0.0033	24.97	19.79	0.39	0.0020	—	—	—	0.026	0.0074	—
		0.065	0.84	1.63	0.024	0.0007	24.78	19.58	0.40	0.028	—	0.0042	—	0.041	0.0058	—
		0.060	0.85	1.65	0.025	0.0007	24.68	19.56	0.40	0.024	—	—	—	0.037	0.0054	—
	Commercial CC slab	0.060	0.77	1.56	0.024	0.0015	24.25	19.45	0.40	0.005	—	—	—	0.031	0.0051	—
0.060		0.77	1.56	0.024	0.0015	24.25	19.45	0.40	0.005	—	—	0.030	0.031	0.0051	—	
Duplex	50 kg ingot	0.012	0.51	1.05	0.027	0.0007	22.2	5.48	3.0	0.048	—	—	—	0.13	—	—
		0.015	0.52	1.06	0.025	0.0043	22.1	5.49	3.0	0.042	—	—	—	0.14	—	—
		0.012	0.76	1.52	0.008	0.0068	21.2	4.90	2.8	0.005	—	—	—	0.12	—	—

\*  $\delta_{\text{est}} = 3.2(1.5\text{Si} + \text{Cr} + 6\text{Al} + 0.5\text{Nb}) - 2.5(30\text{C} + 30\text{N} + 0.5\text{Mn} + \text{Ni}) - 24.7$

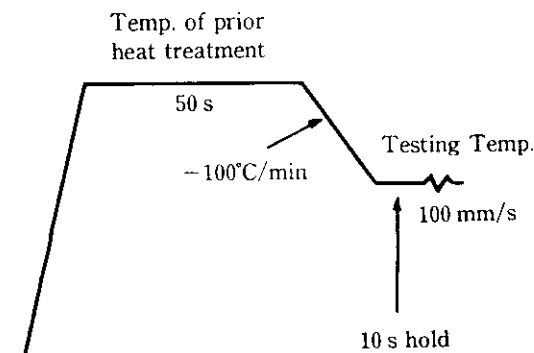


Fig. 1 Heat pattern of Gleeble tensile test

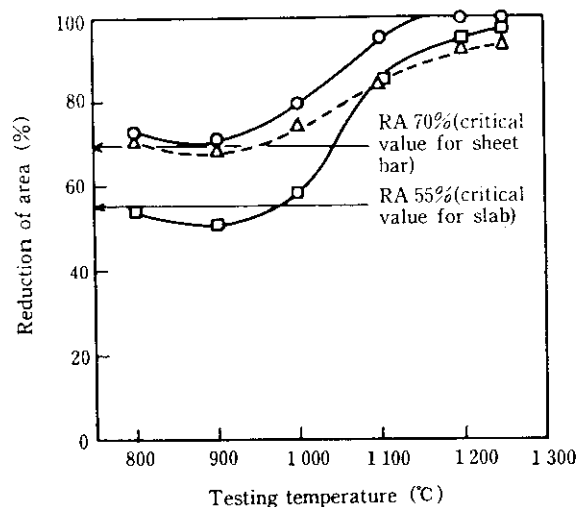
tensile direction was parallel to the casting direction. Rolled specimens were cut so that tensile direction was parallel to the rolling direction. Blocks from as-cast and hot rolled specimens were heat treated for 2 and 1.5 hours, respectively, prior to machining. Most blocks were heat treated at 1250°C. Figure 1 shows the heating pattern of the Gleeble test. Test pieces were rapidly heated to the temperature at which blocks had been heated previously, then held at that temperature for 50 seconds, and next cooled to the testing temperature at a rate of 100°C/min. After the pieces had been held for 10 seconds at the testing temperature to ensure uniformity of heating, they were stressed to fracture at a tensile rate of 100 mm/s. The strain rate was about  $5 \text{ s}^{-1}$ .

Microstructures of heat-treated specimens and fractured test pieces were observed by optical microscope in a cross section parallel to the rolling or casting direction, with  $\delta$ -ferrite dark-etched with a sodium pyrosulfite etching reagent. Amounts of  $\delta$ -ferrite were evaluated by areal percentage as measured by QTM (Quantitative Television Microscope).

### 3 Results

#### 3.1 Evaluation of Hot Ductility

The influence of high hot ductility values on the control and elimination of cracking was studied in the high-temperature high-speed tensile test as a means of determining measures for actual production processes. Figure 2 shows temperature dependence of  $RA$  of materials for which cracking assessments were obtained in the actual process. Sheet bar samples obtained at the roughing mill with  $RA$ 's higher than 70% did not crack at the finishing mill; on the contrary, however, those with  $RA$ 's below 70% showed edge cracks of about 5 mm. Heat cycles in this test were slightly different from those in the actual process, in which finishing roll-



	mark	alloy	result
90% rolled sheet bar sample	○	20Cr-10Ni	OK
	△	22Cr-11Ni	edge crack (<10 mm)
Slab sample	□	17Cr-7Ni	edge crack (<10 mm)

Fig. 2 Comparison between the results in hot rolling into strip and the hot workability obtained by tensile test

ing immediately follows roughing. Here, the sheet bar samples were cooled once and heated again for the test. However, this difference may have no great effect, since roughing is performed at the recrystallization range of 1100°C or higher. Thus, for hot deformed materials of homogeneous structure, 70%  $RA$  is the critical value above which edge cracking during hot rolling will not occur. In contrast, for CC slab samples, this critical value is estimated at about 55%. Consequently,  $RA \geq 55\%$  should be a target for as-cast slabs when soaking, sizing deformation, and heat treatment are performed. However, specimens with as-cast structures or slightly deformed ones usually exhibit bad fracture shape when ductility is low, and results of  $RA$  are often scattered. Therefore, it is helpful, if effects of alloying components, impurities, or added elements are to be examined,  $RA$  values are measured for samples with hot rolled homogeneous structures and, as well, conditions to raise  $RA$  to 70% or larger are determined.

#### 3.2 Hot Ductility of Austenitic Stainless Steels

Figure 3 shows the effect of S on the temperature dependence of hot ductility in 17-7 PH stainless steel. Hot ductility is improved, both in steel with as-cast structure and with hot-rolled structure, when S contents decrease. This effect is particularly marked at temperatures higher than that at the end of hot rolling, or about 900-1000°C. However, even when the content of S is

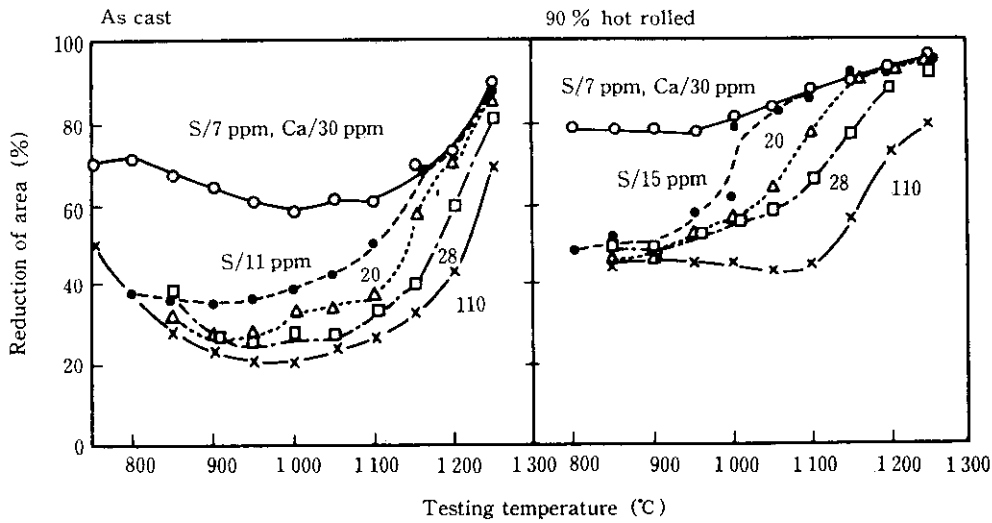


Fig. 3 Effect of S on the hot workability of 17-7 PH stainless steels with as-cast and hot worked structures

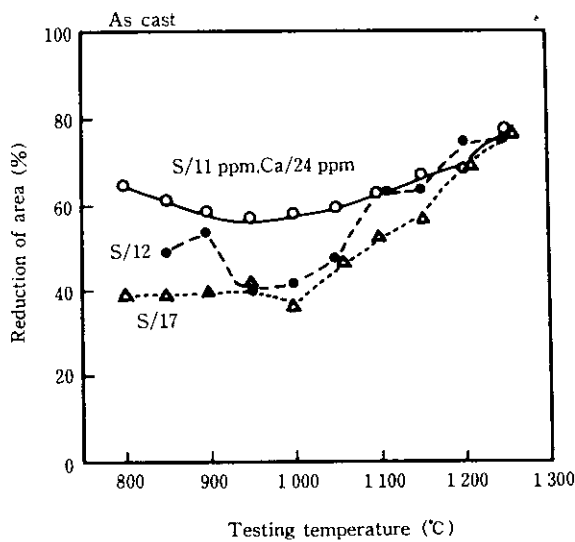


Fig. 4 Effect of S and Ca on the hot workability of KWB 309 NB (23Cr-13Ni-1Nb)

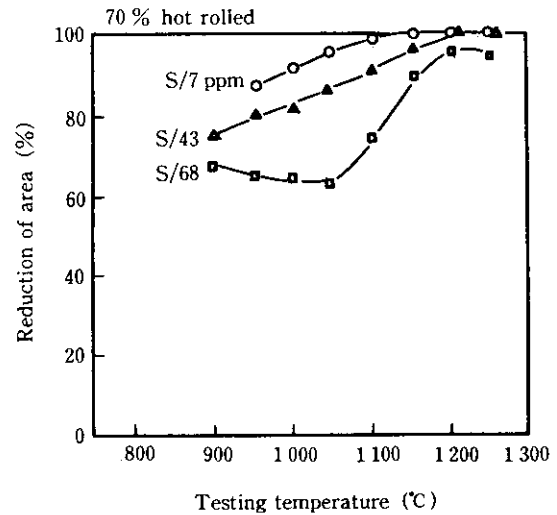


Fig. 5 Effect of S on the workability of duplex stainless steel (22Cr-5Ni-3Mo)

lowered to around 10 ppm, the minimum value of *RA* of as-cast material is smaller than 40% and that of rolled material is 50%, and edge cracking cannot be avoided. On the contrary, in materials with S contents lowered as far as possible and Ca added to stabilize S, ductility is improved remarkably, even in the low temperature range, and becomes comparable to that of conventional SUS 304. In this case, the problem of cracking in rolling does not occur.

Figure 4 shows results with an overlay electrode material KWB309NB and Fig. 5, those with  $\alpha$ - $\gamma$  duplex stainless steel. Although KWB309NB contains Nb, results are about the same as those with 17-7 PH stainless steel when S content is decreased and stabilized. It is clear that edge cracking in hot rolling can be avoided in

$\alpha$ - $\gamma$  duplex stainless steels by reducing S content to around 40 ppm. Thus, a duplex stainless steel consisting almost entirely of  $\delta$ -phase at high temperatures shows little of the detrimental effect of S seen in other duplex steels having about 30%  $\delta$ -ferrite, and can be rolled with relative ease.

Figure 6 shows results with SUS 310S consisting of  $\gamma$ -phase alone. In this case, as above, ductility is remarkably improved by reducing only the S content. This material is characterized by the fact that the reduction in *RA* due to S is limited to a temperature range in the vicinity of 1050°C. This behavior can also be seen in  $\gamma$  single phase steels such as SUS 316L. When ductility shows such temperature dependence, cracking occurs on the center surface in the initial rolling stage, and

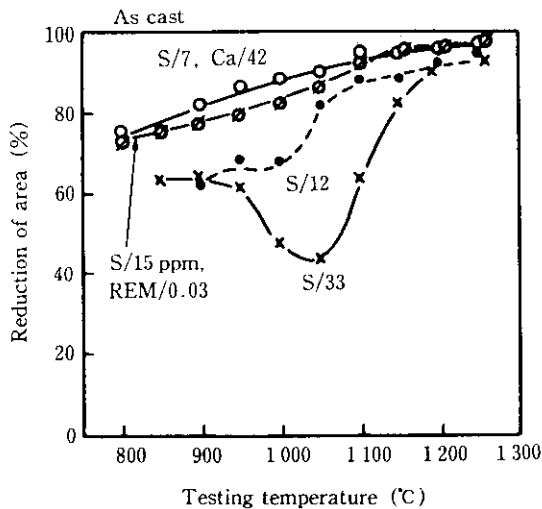


Fig. 6 Effect of S and addition of Ca or REM on the hot workability of type 310S stainless steel

these cracks become sliver defects in hot strip. In this case, edge cracks which can be observed at low temperature portions in materials containing  $\delta$ -phase do not occur. Also in the case of  $\gamma$  single phase steels, ductility is markedly improved when S content is greatly reduced and stabilized. Ca and REM are considered to have the same effect in stabilizing S.

## 4 Discussion

### 4.1 Effect of S on Hot Ductility

Many reports describe the detrimental effect of S.<sup>2)</sup> On the other hand, according to the results described above, hot ductility can be improved and cracking avoided by extreme reduction of S content. S content, however, must be decreased to a level much lower than previously thought sufficient, particularly with austenitic stainless steels containing  $\delta$ -ferrite. Further, as shown in Fig. 7, ductility can be remarkably improved by stabilizing S, even when the content of S is 10 ppm or smaller. Large amounts of Ca or REM cannot be added in the actual process, and even if this were possible, it might cause other problems, such as surface defects. For this reason, it is desirable to add these elements after the content of S has been reduced to a very low level. When Ca is added to improve ductility, the value of Ca/S must be 3 or larger, as shown in Fig. 8.

As stated above, S seriously affects hot ductility even at levels lower than 10 ppm. A mechanism has been suggested to explain the fact that S reduces ductility: dissolved MnS or (MnFe)S at high temperature reprecipitates finely or segregates on the grain boundary as the temperature drops during hot rolling and thus weakens the strength of the grain boundary.<sup>3,4)</sup> In this mecha-

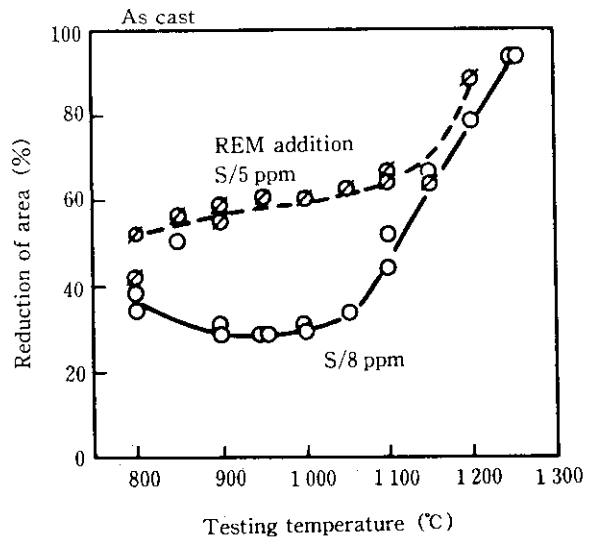


Fig. 7 Effect of REM addition to ultra low S steel on the hot workability of KWB 309 (22Cr-9Ni)

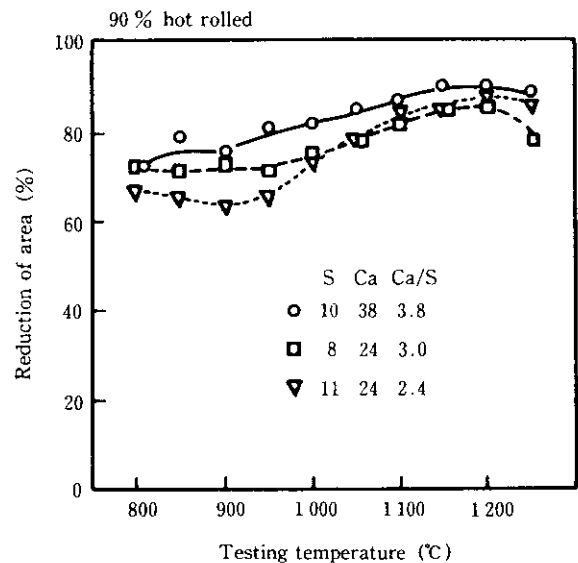


Fig. 8 Effect of S and Ca on the hot workability of KWB 309 NB (23Cr-13Ni-1Nb)

nism, MnS simply coarsens at relatively low heating temperature, where its solubility is low, and then only cleans the grain boundary. Therefore, S is not detrimental when the heating temperature is low. However, the higher the heating temperature, the greater the increase in solubility and, accordingly, the greater the reduction in ductility during the cooling process. Figure 9 clearly shows this fact. This is because 17-7 PH stainless steel contains 20 ppm S. In this figure, RA's at heating temperatures of 1 200°C and 1 300°C differ by about 20% over almost the entire temperature range. Since only heating temperatures were changed in this experiment,

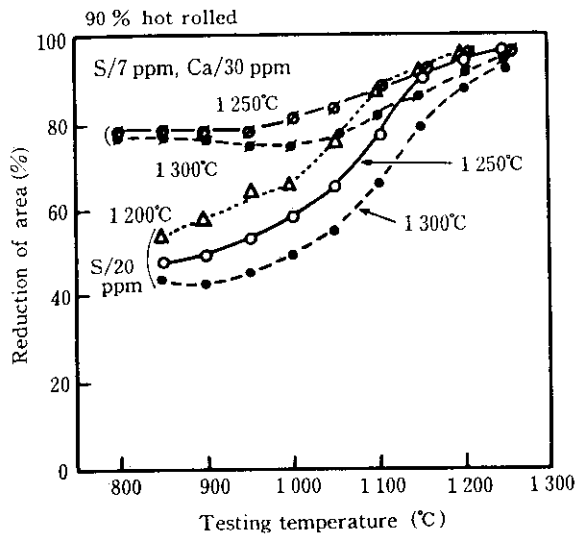


Fig. 9 Effect of heating temperature prior to Gleeble tensile test on the hot workability of 17-7 PH stainless steel

it is possible to conclude that 20 ppm of S affects hot ductility due to its dissociation and precipitation. Added Ca may be considered to stabilize and prevent S from dissolving and re-precipitating. Exactly speaking, it is thought that CaS is partly dissolved because ductility decreases slightly at a 1300°C heating temperature. From this finding, it can also be concluded that it is necessary to lower the absolute content of S even when Ca is added.

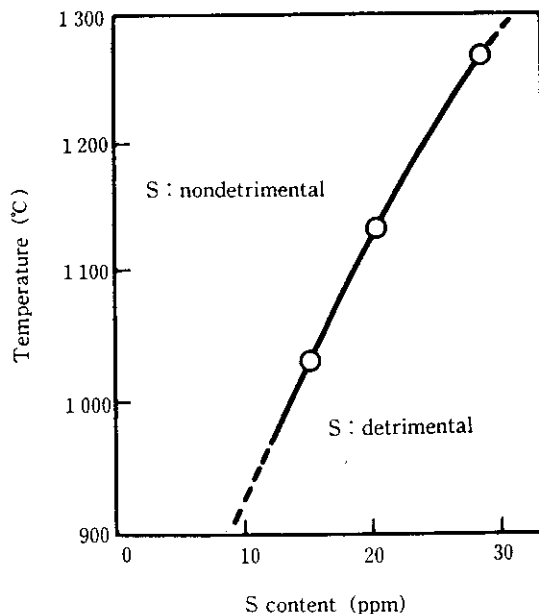


Fig. 10 Relation between S content and critical temperature, above which S has no effect on the hot workability

Assuming that the effect of S can be disregarded in steel in which S is stabilized by Ca, then, in the cooling process, it may be considered that the temperature below which the ductility of steels containing unstabilized-S is lower than that of steels containing stabilized-S is the apparent temperature at which detrimental MnS begins to precipitate. Figure 10 shows the relation between S content and this apparent precipitation temperature estimated from results with the rolled steels shown in Fig. 3. The extrapolation of this graph shows that S should be reduced to a content lower than 10 ppm to completely eliminate the effect of S when 17-7 PH stainless steel is to be heated to 1250°C and hot rolled. According to the results in Fig. 9, it is expected that this apparent solubility line will shift to the high temperature side, that is, low S content side, when higher heating temperatures are applied.

#### 4.2 Effect of $\delta$ -Ferrite Shape on Hot Ductility

As can be seen from Fig. 3, the ductility of hot rolled steels is higher than that of as-cast ones. This is considered to be a result of a reduction of segregation in casting and the homogenization of the microstructure. To confirm these points, the effect of  $\delta$ -ferrite shape on hot ductility was investigated with as-cast CC slab of 17-7 PH stainless steel. The shape of  $\delta$ -ferrite in the as-cast microstructure was altered by hot rolling and heat treatment for homogenization. Applied treatments were as follows:

- A: 1250°C, 2 h heating
- B: 1250°C, 2 h heating, 35% rolling + 1250°C 2 h heating
- C: 1200°C, 10 h soaking for homogenization + 1250°C, 2 h heating
- D: 1250°C, 2 h heating, 35% rolling + 1200°C, 10 h soaking for homogenization + 1250°C, 2 h heating

Photo 2 shows microstructures observed by optical microscope following these various treatments. The shape of  $\delta$ -ferrite varies depending on the combination of rolling and heat treatment. When both treatments are applied,  $\delta$ -ferrite is dispersed in a fine, homogeneous manner. The microstructure with treatment A shows  $\delta$ -ferrite of a continuously elongated shape, in a slightly larger amount than that with treatments B, C, and D, which have almost equal amounts of the phase. Figure 11 shows the hot ductility of materials having the above microstructures. It is clear that the slab soaked at 1200°C has better hot ductility below 900°C than that of the as-cast slab which was only heated. The ductility of 35% hot rolled slab is improved except in the vicinity of 950°C, and that of slab which has been both hot rolled and soaked is improved over the whole temperature range. Although a hot rolling process which does not improve ductility between 900 and 1000°C is not practical for preventing edge cracking, performing both hot

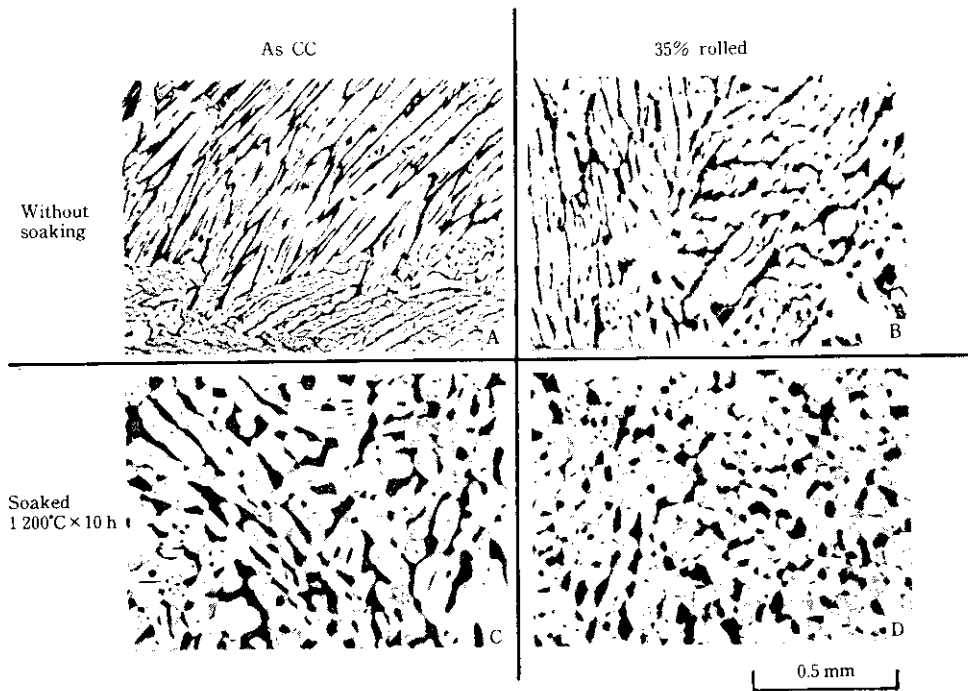


Photo 2 Change in shape of  $\delta$ -ferrite of 17-7 PH stainless steel after thermal and mechanical treatment ( $\delta$ -ferrite %: A, 20.7; B, 15.4; C, 14.4; D, 14.9)

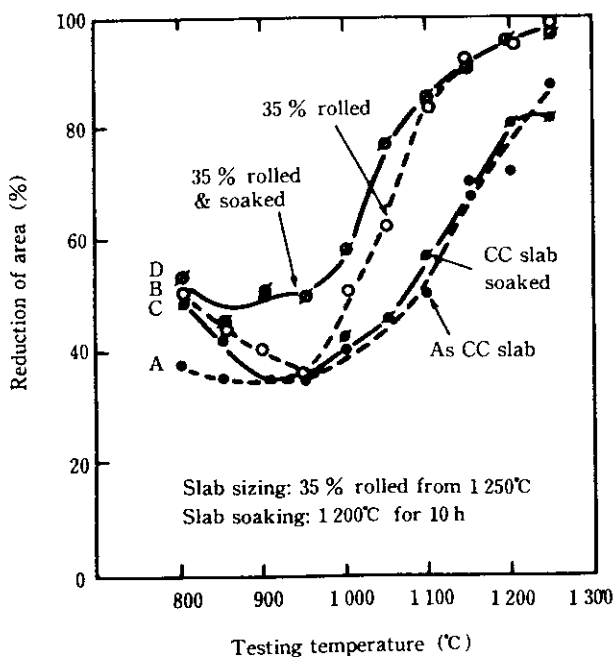
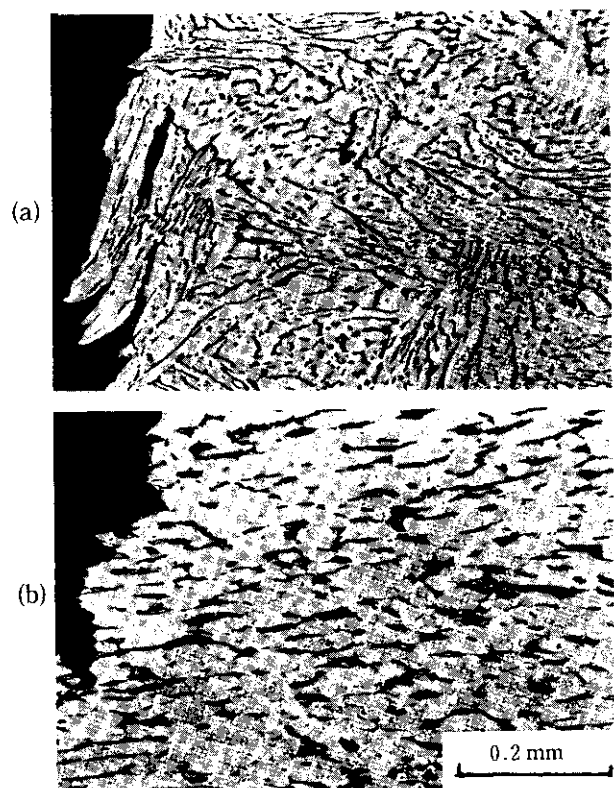


Fig. 11 Effect of thermal and mechanical treatment on the hot workability of 17-7 PH stainless steel



(a) Elongated  $\delta$ -ferrite  
 (b) Fine-homogeneously dispersed  $\delta$ -ferrite  
 Photo 3 Microstructures of 17-7 PH stainless steel with different shapes of  $\delta$ -ferrite at fractured position

rolling and soaking can be used effectively. Photo 3 shows sectional microstructures near the fractured portion of test pieces with different  $\delta$ -ferrite shapes fractured at 1050°C. Deformation is concentrated at the fractured portion in the material having elongated  $\delta$ -fer-

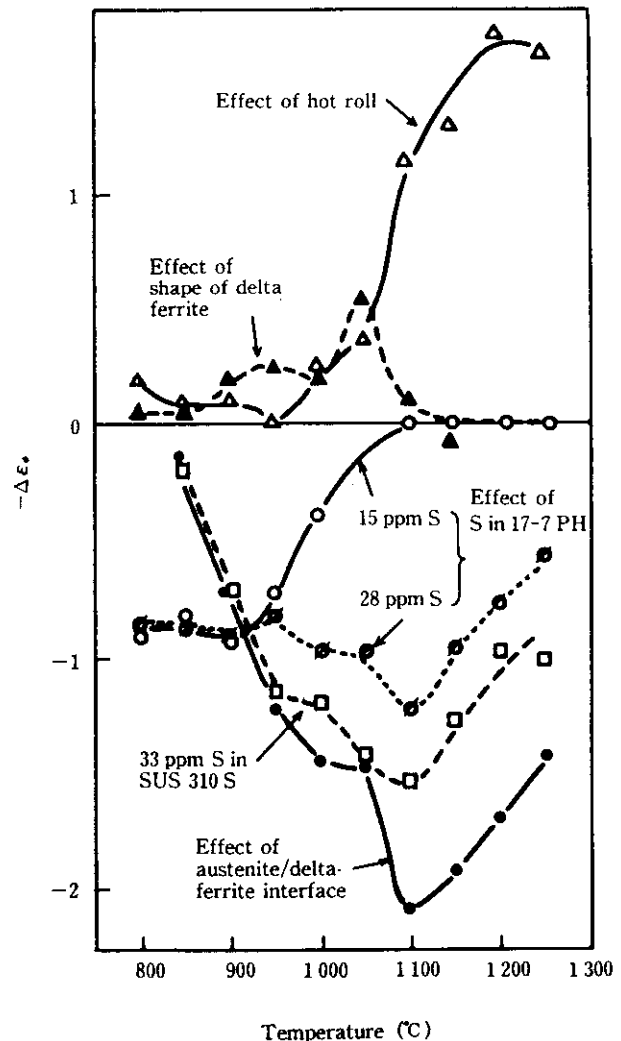


rite. On the other hand, in the material having homogeneously dispersed  $\delta$ -ferrite, deformation occurs over a wide range, and voids can be seen at the  $\alpha$ - $\gamma$  phase boundaries, far from the fractured portion. This means that crack propagation characteristics differ depending on the shape of the  $\delta$ -phase and, therefore, that hot ductility varies. The improvement in ductility at higher temperatures by hot rolling is considered similar to that of S reduction, as shown in Fig. 3, and is thought to be caused by the decrease in segregation of the cast structure.

#### 4.3 Compound Effect of $\delta$ -ferrite and S on Hot Ductility

To clarify the respective effects of  $\delta$ -ferrite and S on hot ductility, ductility was measured at various temperatures in the cooling process for steels containing (a)  $\delta$ -ferrite, (b) no  $\delta$ -ferrite, (c) Ca-stabilized S, and (d) unstabilized S. *RA* of each steel was expressed as logarithmic strain as a basis for evaluating the difference between (a) and (b), and (c) and (d). Figure 12 shows results obtained. In this figure, the higher the value of ductility difference  $-\Delta\epsilon_\phi$ , the larger the ductility. When there is no detrimental effect of S, the difference originating in the  $\gamma$ - $\delta$  phase boundary is calculated from values of 17-7 PH and 310S, in which S is stabilized. The ductility reduction is greatest at 1 100°C, and the effect of the  $\gamma$ - $\delta$  phase boundary disappears as temperature drops. The difference originating in S contained in  $\gamma$ -phase is calculated from values of Ca-added 310S and Ca-free 310S. The detrimental effect of S is greatest at 1 100°C, as with  $\gamma$ - $\delta$  phase boundary. These facts mean that  $\delta$ -phase and S contained in  $\gamma$ -phase do not act independently to reduce ductility at about 1 100°C when they do not exist simultaneously. That is to say it is not possible to explain the edge cracking due to temperature decrease by the independent effect of one or the other of these factors.

The effect of S on the ductility of 17-7 PH stainless steel can be seen from the difference between the stabilized-S and unstabilized-S materials. In Fig. 12, results with 90% hot-rolled steel are shown. When the steel includes 28 ppm S, ductility decreases seriously at 1 100°C. This reduction is the same as seen in the steel of  $\gamma$  single phase. However, in this case, recovery of ductility is not observed when temperature drops. On the contrary, ductility is affected by S to almost the same degree at temperatures down to 800°C. In 17-7 PH stainless steel containing 15 ppm S, S has no effect at higher temperatures of 1 050°C. However, ductility drops to the same level as in steel including 28 ppm S when temperature drops below 1 000°C. These results mean that the ductility reduction at lower temperatures is due to the presence of S in conjunction with that of  $\delta$ -ferrite indicating that their effects should be considered interactive.



- ▲ :  $\Delta\epsilon_\phi = \epsilon_\phi(17-7PH, \text{ rolled \& soaked}) - \epsilon_\phi(17-7PH, \text{ rolled})$
- △ :  $\Delta\epsilon_\phi = \epsilon_\phi(17-7PH, \text{ rolled}) - \epsilon_\phi(17-7PH, \text{ as CC})$
- :  $\Delta\epsilon_\phi = \epsilon_\phi(17-7PH, \text{ S free}) - \epsilon_\phi(310S, \text{ S free})$
- :  $\Delta\epsilon_\phi = \epsilon_\phi(310S, 30 \text{ ppmS}) - \epsilon_\phi(310S, \text{ S free})$
- :  $\Delta\epsilon_\phi = \epsilon_\phi(17-7PH, 28 \text{ ppmS}) - \epsilon_\phi(17-7PH, \text{ S free})$
- ◇ :  $\Delta\epsilon_\phi = \epsilon_\phi(17-7PH, 15 \text{ ppmS}) - \epsilon_\phi(17-7PH, \text{ S free})$

Fig. 12 Temperature dependence of hot workability difference in steels compared with S free or  $\delta$ -ferrite free steels (Hot workability difference is evaluated by the difference of log strain converted from reduction of area)

Figure 12 also shows the contribution of hot rolling and soaking to slab ductility. Hot rolling is effective only above 1 000°C, while fine-homogenization of  $\delta$ -ferrite by rolling and soaking is effective at between 900 and 1 100°C.

As shown in Fig. 13,<sup>1)</sup> the amount of  $\delta$ -ferrite affects hot ductility, with ductility reaching its minimum level at 10-30%  $\delta$ -ferrite. S contents of specimens shown in this figure were not clear, but hot ductility was lower

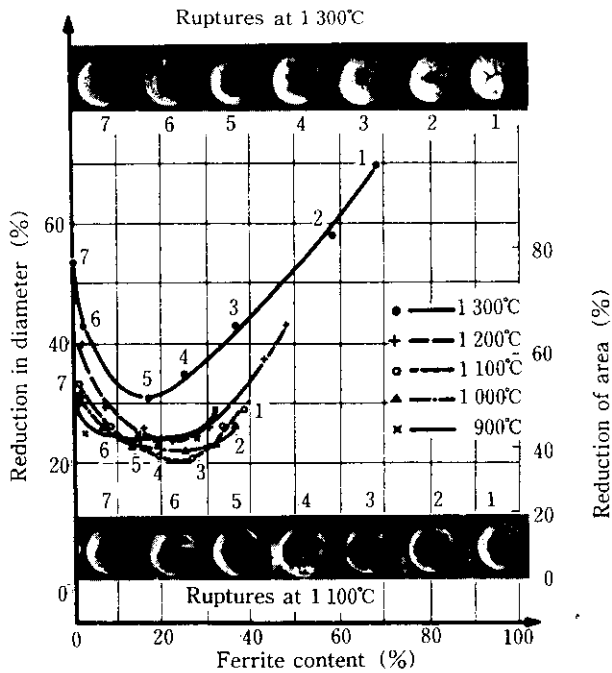


Fig. 13 Effect of  $\delta$ -ferrite content on the hot workability of Fe-Cr-Ni alloys with columnar cast structure<sup>1)</sup>

than that reported here for extremely low S and Ca-stabilized steels. However, as can also be seen in this investigation from Figs. 3-6, the dependence of  $\delta$ -ferrite amount on hot ductility may be expected to appear as a concave curve. Generally speaking, the amount of  $\delta$ -ferrite decreases during cooling, meaning that the action of S and the effect of the amount of  $\delta$ -ferrite overlap in the cooling process. Since no accurate phase diagram for 17-7 PH stainless steel has been devised, the change in the amount of  $\delta$ -ferrite was investigated, using the same heat treatment conditions as were used in the high-temperature high-speed tensile test. As shown in Fig. 14,  $\delta$ -ferrite with an initial value of about 35% at 1 250°C decreases continuously in the cooling process at the rate of 100°C/min to about 15% at 800°C. It is clear from Fig. 13 that as the temperature drops, the amount of  $\delta$ -ferrite changes to that at which ductility is lowest. Further, as can be seen in Fig. 13, ductility remains at the same level at below 1 200°C. However, as shown in Fig. 3, ductility is recovered at lower temperatures by Ca addition; therefore, this recovery cannot be explained simply on the basis of changes in the amount of  $\delta$ -ferrite. When  $\delta$ -ferrite exists in  $\gamma$ -phase, austenite formers are considered to be enriched in  $\gamma$ -phase and ferrite formers in  $\delta$ -ferrite. It is thought that S is enriched in  $\delta$ -ferrite,<sup>5)</sup> then sulfide dissociation and precipitation affected not only by temperature change but also by  $\delta$ -ferrite decrease. The reduction of  $\delta$ -ferrite is promoted by the encroachment of  $\gamma$ -phase of lower S content upon  $\delta$ -ferrite of

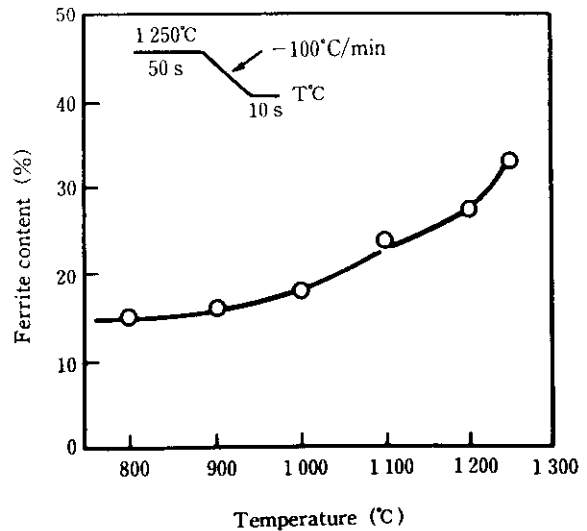


Fig. 14 Change in the amount of  $\delta$ -ferrite of 17-7 PH stainless steel cooled from 1 250°C at a rate of -100°C/min

larger S content, so that S is expelled from  $\delta$ -ferrite and concentrated at the boundary. **Photo 4** shows the void formation near the fractured portion of 17-7 PH stainless steel (28 ppm S) tensile-tested at 1 050°C. Cracking is initiated by exfoliation at the phase boundary and in the area where  $\gamma$ -phase seems to have encroached on  $\delta$ -ferrite. **Figure 15** shows this mechanism schematically. If the fine sulfide-precipitation mechanism is correct, precipitates should be observed in the  $\gamma$ - $\delta$  boundary, but, as of this investigation, have not been detected by electron microscopy.

It is thought that the hot ductility reduction of austenitic stainless steels is caused by reasons such as the boundary slip of coarsened  $\gamma$ -grains,<sup>6)</sup> void formation due to deformation caused by transformation from  $\delta$  to



Photo 4 Crack initiation at austenite/ $\delta$ -ferrite phase boundary

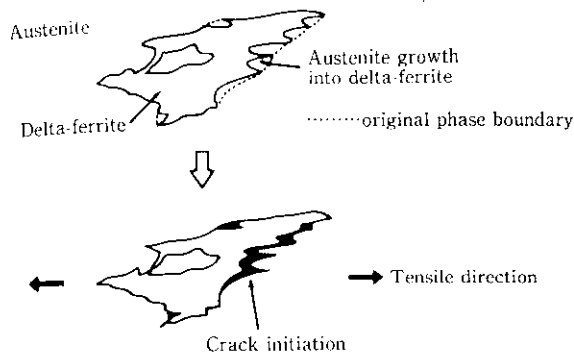


Fig. 15 Schematic representation of crack initiation

$\gamma$ ,<sup>7)</sup> precipitation of carbides such as NbC,<sup>8)</sup> and the effect of P or O. However, since specimens used in this investigation had constant levels of impurity elements, except S and S-stabilizer, it is difficult to give a cogent explanation of ductility changes on the basis of the thinking stated above. At extremely low S levels, it is also appropriate to consider the simultaneous effects of S and  $\delta$ -ferrite.

## 5 Conclusions

The hot ductility of austenitic stainless steels containing  $\delta$ -ferrite, which present problems of edge cracking in hot rolling, have been investigated with the following conclusions.

- (1) Hot ductility is seriously affected by S, so the edge cracking in conventional hot rolling can be prevented only if the detrimental effect of S is eliminated. To accomplish this, S must be decreased to 10 ppm

or lower, or extremely reduced S must be stabilized by Ca or REM.

- (2) Ductility reduction due to  $\delta$ -ferrite occurs in the temperature range around 1100°C, as is also the case with S.
- (3) When  $\delta$ -ferrite and S exist together, the range of ductility reduction extends to lower temperatures, and this causes edge cracking.
- (4) Finely and homogeneously dispersed  $\delta$ -ferrite provides better ductility than elongated and linked  $\delta$ -ferrite, and is also effective in the lower temperature range.

## 6 Appendix

In this investigation, sodium pyrosulfite solution was used as etching reagent for microstructure observation. The  $\delta$ -ferrite etched with this solution becomes black, making this etchant convenient and effective for QTM phase ratio measurement.

The composition of the solution is as follows:

Solution I	{	Methanol	100 ml
		Nitric acid	25 ml
		Chloric acid	25 ml
Solution II	{	Distilled water	100 ml
		Sodium pyrosulfite (Na <sub>2</sub> S <sub>2</sub> O <sub>5</sub> )	1.5 g

In etching, solution I and II are mixed in equal amount, and the specimen to be etched is immersed for 5-60 seconds at room temperature in this mixed etchant. **Photo A** shows the difference between etched

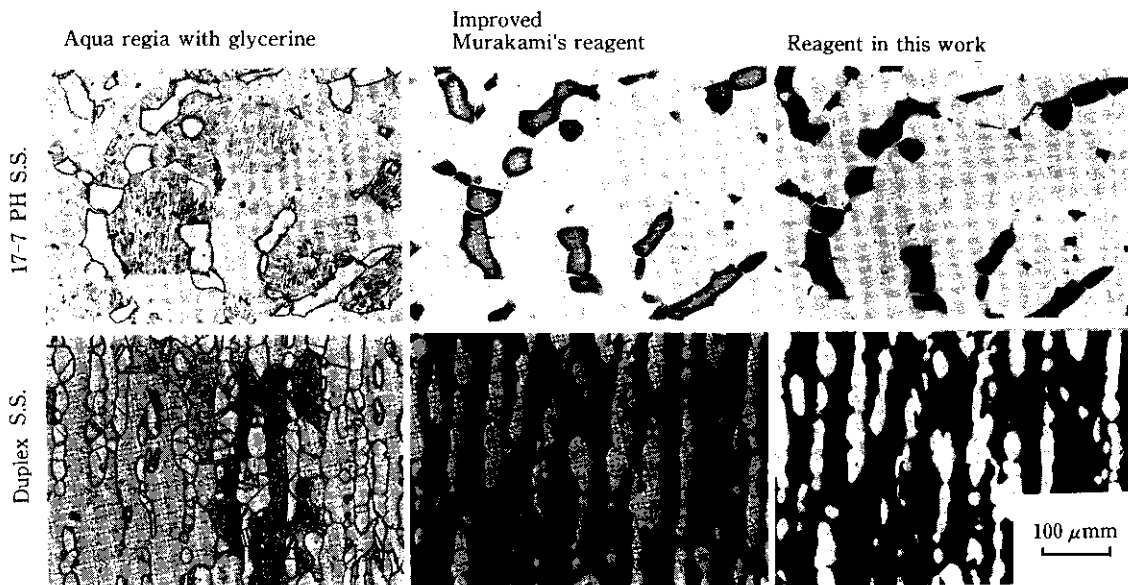


Photo A Comparison of etched structures

microstructures with aqua regia with glycerine, improved Murakami's reagent, and the reagent described above.

#### References

- 1) J.H. Decroix, A.M. Neveu and R.J. Castro: Proceedings of the conference on "Deformation Under Hot Working Conditions," The Iron and Steel Institute, (1968), 135
- 2) H. Sudo: "Metallurgy of Steels under Hot Work Deformation," Final report of the High Temperature Deformation Committee, Organization of Joint Society on Iron and Steel Basic Research, ISIJ, (1982), 249
- 3) H. Suzuki, T. Nishimura, and S. Yamaguchi: *Tetsu-to-Hagané* 65(1979)14, 2023
- 4) T. Ishiguro: "Metallurgy of Steels under Hot Work Deformation," Final report of the High Temperature Deformation Committee, Organization of Joint Society on Iron and Steel Basic Research, ISIJ, (1982), 357
- 5) H. Sudo: "Deformation Behavior of Iron and Steel at Elevated Temperature," Report of the High Temperature Deformation Committee, Organization of Joint Society on Iron and Steel Basic Research, ISIJ, (1979), 97
- 6) H. Suzuki, S. Yamaguchi: *ibid.*, (1979), 113
- 7) M. Saito, M. Imamura, and Y. Itoh: "Metallurgy of Steels under Hot Work Deformation," Final report of the High Temperature Deformation Committee, Organization of Joint Society on Iron and Steel Basic Research, ISIJ, (1982), 274
- 8) H. Kobayashi, S. Yamaguchi, and M. Endo: Proceedings of the conference on "Hot Working and Forming Processes," The Metals Society, London, (1979), 133